An Eigenvector Method for the Calculation of Directional Spectra from Heave, Pitch and Roll Buoy Data

R. F. MARSDEN

Department of Physics, Royal Roads Military College, FMO, Victoria, B.C., Canada V0S 1B0

B.-A. JUSZKO*

Seakem Oceanography Ltd., Sidney, B.C., Canada V8L 3S1

(Manuscript received 15 September 1986, in final form 4 May 1987)

ABSTRACT

An eigenvector (EV) method for the determination of directional spectra from heave, pitch and roll buoy data is presented. Both a direct and an iterative form (based on an algorithm by Pawka) of this data-adaptive procedure are developed. The direct form outperforms the Longuet-Higgins et al. method, the cosine spread model and the maximum likelihood (ML) method for both simulated and real data. In the iterative form, the iterative EV method is superior to the other methods tested, including the iterative ML method for unimodal peaks when the noise-to-signal ratio is greater than 0.2 and for bimodal peaks at all noise levels. With real data, the direct EV method produced errors within an 80% confidence zone of the data cross-spectral matrix within the stopping criteria of Lawson and Long. Errors of the iterative EV and iterative ML methods were lower than for both the direct EV and ML results and were about the same magnitude when compared to each other. The iterative EV method, however, produced narrower, more sharply defined unimodal and bimodal spectra.

1. Introduction

For nearly twenty years, heave, pitch and roll buoys have offered an attractive operational means to determine wave directional spectra. For a moderate cost, the buoy can be deployed at a remote single location, the wave information can be telemetered to recording instruments and the results can be used to give time series of the sea-surface directional spectra. Although the mechanical configuration of the sensor may vary, essentially one obtains estimates of the wave amplitude and directional derivatives of the sea surface as a function of time. By far the most commonly used analysis of the data was proposed by Longuet-Higgins et al. (1963). Here the directional spectrum is expanded in a Fourier series which is truncated at second order and the coefficients are fit to the elements of the cross-spectral matrix of the amplitude and two slopes. This technique has several disadvantages. First, a direct application of the method can result in negative spectral energy densities. An arbitrary weighting function must be applied to correct this deficiency and hence the resulting spectrum is not unique. As Longuet-Higgins et al. (1963) state: "Other weighting functions of course are possible; which particular function one chooses is to some extent a matter of taste." Second, the resulting spectrum is broad-banded; consequently, waves from two different directions at the same frequency cannot be resolved. Another major approach is to select mathematical functions a priori to model the directional distribution of wave energy. Prevalent among these is the cosine-spread model in which the Longuet-Higgins parameters are fit to a cosine function raised to a (varying) power. One is restricted here, however, to resolving symmetric unidirectional distributions.

An alternative analysis is an inverse technique outlined by Lawson and Long (1983). It is an extension of an iterative inverse technique designed for multielement arrays proposed in Long and Hasselmann (1979). This approach does resolve two directions at the same frequency (i.e. bimodal distributions) and implicitly requires the calculation of the estimated error between the model and directly measured cross-spectral matrix. The resulting directional spectrum, however, is weakly dependent on an a priori chosen favored direction distribution, and the iteration is quite complex to implement. Davis and Regier (1977) have described several data adaptive techniques based on the maximum likelihood (ML) method for calculating the directional spectra for arrays of wave detectors. Oltman-Shay and Guza (1984) have proposed an iterative technique based on the ML method that increases the directional resolution of heave, pitch and roll buoys. In this paper, we propose a generalized version of the ML technique in which the data are partitioned into signal and noise components determined by the eigenvalues of the cross-

* Present address: 483 Sue Mar Pl., Victoria, B.C., Canada V9C 3E1.

spectral matrix. The method is data adaptive, and in its direct form gives a resolution superior to other direct methods tested; for the majority of frequencies it also produces errors in the estimated cross-spectral matrix within the minimization criteria of Lawson and Long (1983). The method is also adaptable to the iterative scheme of Pawka et al. (1984), and in this form shows superior resolution of bimodal spectra.

2. Theory

Let the measured wave amplitudes and slopes be described as $\eta_i(t)$ where $i = 1$ is the vertical displacement of the sea surface from the undisturbed state, $i = 2$ is the east slope positive up and $i = 3$ is the north slope positive up. An estimate of the cross-spectral matrix can be calculated as

$$\hat{Q}_{ij}(\omega) = \frac{1}{2\pi}\int_{-T/2}^{T/2} \langle \eta_i(t)\eta_j(t+\tau)\rangle e^{-i\omega\tau} d\tau \qquad (1)$$

where $\langle \eta_i(t)\eta_j(t+\tau)\rangle$ is the covariance between the ith and jth data type at lag τ, and T is duration of the sample. The caret indicates that the estimate of the cross-spectrum results from a band-limited sampling. A signal consisting of a plane wave of infinite duration and wavenumber k traveling from a direction θ can be described by

$$\zeta_i = A\beta_i e^{i[k(x\cos\theta + y\sin\theta) - \omega t]} \qquad (2)$$

where $\beta = (1, ik\cos\theta, ik\sin\theta)$ is commonly called the look vector in acoustic beamforming theory. A measurement will consist of a signal and a noise component

$$\eta_i = \zeta_i + \epsilon_i \qquad (3)$$

where ϵ_i is the noise. The noise can arise from geophysical effects where the plane wave assumption is not valid, from inherent instrument error, and from statistical uncertainty due to sampling a finite quantity of data. Furthermore, the power estimate at any particular direction may be affected by adjoining wavenumbers due to spectral "leakage".

For the maximum likelihood (ML) estimate, it is assumed that an estimate of the heave amplitude can be constructed from a linear combination of the data elements

$$\hat{\zeta}_1 = \sum \gamma_i^* \eta_i. \qquad (4)$$

The directional spectrum is then given by

$$\hat{E}(\theta) = \langle \hat{\zeta}_1 \hat{\zeta}_1^* \rangle = \gamma^* \hat{Q} \gamma. \qquad (5)$$

Here, γ is a vector of filter coefficients which when applied to the input signal estimates, results in the true amplitude signal. The asterisk ($*$) represents complex conjugation and the brackets denote an ensemble average of a number of realizations of the spectral estimate. If the signal consists purely of a plane wave with no noise, Eq. (4) becomes

$$\zeta_1 = \sum \gamma_i^* \zeta_i$$

or

$$\gamma^* \beta = 1. \qquad (6)$$

Equation (5) is minimized subject to the constraint that a pure plane wave signal be filtered with unit gain [i.e. Eq. (6)] by Lagrange's method of undetermined multipliers. The result is

$$\hat{\mathbf{E}}(\theta) = \frac{1}{(\beta^* \mathbf{Q}^{-1} \beta)}. \qquad (7)$$

The development of the ML technique is standard. Capon (1969) gives an extensive discussion of the technique in a geophysical context and describes the relationship of the method to the likelihood function. Kanasewich (1981) describes the minimization procedure.

An eigenvector (EV) method has been proposed for acoustic wave detection. It is assumed that the cross-spectral matrix can be partitioned into noise and signal components

$$\hat{\mathbf{Q}} = \hat{\mathbf{S}} + \hat{\mathbf{N}} \qquad (8)$$

where $\hat{\mathbf{S}}$ is an estimate of the signal component of the cross-spectral matrix and $\hat{\mathbf{N}}$ is an estimate of the noise component of the cross-spectral matrix. The directional spectrum is again given by Eq. (5) subject to the constraint of Eq. (6). Now, however, only the estimate of the noise component of the directional spectrum is minimized viz

$$\delta^2 = \gamma^* \mathbf{N} \gamma + \lambda(\gamma^* \beta - 1).$$

The result is

$$\gamma = \frac{\hat{\mathbf{N}}^{-1}\beta}{\beta^* \hat{\mathbf{N}}^{-1}\beta}$$

which upon substitution into Eq. (5) gives a spectral estimate of

$$\hat{\mathbf{E}}(\theta) = \frac{\beta^* \hat{\mathbf{N}}^{-1} \hat{\mathbf{Q}} \hat{\mathbf{N}}^{-1} \beta}{(\beta^* \hat{\mathbf{N}}^{-1} \beta)^2}. \qquad (10)$$

The partitioning of the noise and signal components is achieved through the diagonalization of the cross-spectral matrix. If there are n sensors, the p eigenvectors corresponding to the largest eigenvalues are assumed to span the signal while the n–p eigenvectors corresponding to the n–p smallest eigenvalues are assumed to span the noise of the process. The data cross-spectral matrix is then partitioned as

$$\hat{Q}_{ij} = \sum_{l=1}^{p} \lambda_l \phi_i^l \phi_j^{l*} + \sum_{m=p+1}^{n} \lambda_m \phi_i^m \phi_j^{m*} = \hat{\mathbf{S}} + \hat{\mathbf{N}} \qquad (11)$$

where λ are the eigenvalues ($\lambda_1 > \lambda_2 \cdots$) and ϕ are the corresponding eigenvectors. Since the noise cross-spectral matrix is orthogonal to the signal component, Eq. (10) reduces to

$$\hat{\mathbf{E}}(\theta)=\frac{\beta^*\hat{\mathbf{N}}^{-1}(\hat{\mathbf{S}}+\hat{\mathbf{N}})\hat{\mathbf{N}}^{-1}\beta}{(\beta^*\hat{\mathbf{N}}^{-1}\beta)^2}=\frac{1}{\sum_{m=p+1}^{n}\frac{1}{\lambda_m}|\beta^*\cdot\phi^m|^2}. \quad (12)$$

Johnson (1982) derives the EV technique different principles and describes its relation to other acoustic beamforming methods.

The partition between signal and noise is arbitrary. If all the eigenvectors are assumed to span the noise ($p = 0$), the eigenvector (EV) and maximum likelihood (ML) estimates of the directional spectrum are identical. Hence the ML estimate can be considered to be a subset of the EV method. In fact, for this paper the ML-based calculations were computed using the EV algorithm. For heave, pitch and roll buoys, we have only three possible eigenvectors. If only the smallest eigenvector is assumed to span the noise spurious peaks are then introduced into the directional spectra. All EV calculations in this paper use $p = 1$. The selection of signal and noise components is more critical for multicomponent arrays. Barrodale et al. (1985) offer suggestions for determining a suitable partition in this case.

Both the ML and EV techniques were initially introduced as signal detectors. When the number of detectors in the array is small, the results of Pawka (1983) and Pawka et al. (1984) suggest that the ML underestimates the actual spectral power density. The EV method tends to compensate for the underestimation. If the actual signal is a pure plane wave from a direction θ_0, then the eigenvector corresponding to the largest eigenvalue will match the phase and amplitude relations of the wave [i.e., $\phi^1 = \beta(\theta_0) = (1, ik\cos\theta_0, ik \times \sin\theta_0)$]. The other two eigenvectors will be orthogonal to ϕ^1. As $\hat{E}(\theta)$ is evaluated at θ_0 then the denominator of Eq. (12) will go to zero and the estimate of the spectral power density will be infinite. Surface gravity waves, however, have a finite directional spread and for all cases calculated the estimated direction spectrum remained finite. It is not essential that the spectral estimation from Eq. (11) be exact, but rather that the relative amplitudes be correct from one direction to the next. Both the EV and ML spectral estimates were normalized to ensure that the power density was conserved:

$$\hat{Q}_{11}(\omega)=\int_0^{2\pi}\hat{E}(\theta)d\theta \quad (13)$$

where $\hat{Q}_{11}(\omega)$ is the estimated spectral power density at frequency ω.

Pawka (1983) has proposed an iterative technique to improve the resolution of the ML directional estimates. It has been adapted by Oltman-Shay and Guza (1984) for application to pitch and roll type measurements. Let $\hat{E}^i(\theta)$ be a new spectral estimate at direction θ found from

$$\hat{E}^i(\theta)=\hat{E}^{i-1}(\theta)+\epsilon_i(\theta).$$

Pawka calculates the improvement as

$$\epsilon_i=\frac{|\alpha|^{\xi+1}\hat{E}^{i-1}(\theta)}{\alpha\psi} \quad (14)$$

where

$$\alpha = 1.0 - \frac{T^{i-1}(\theta)}{\hat{E}^0(\theta)};$$

$T^{i-1}(\theta)$ is the ML spectrum calculated from the cross-spectral matrix of $\hat{E}(\theta)$ and $\hat{E}^0(\theta)$ is the original ML spectrum. The parameters ξ and ψ control the rate of convergence and in accordance with Oltman-Shay and Guza (1984), values of $\xi = 1.0$ and $\psi = 20.0$ were chosen for this study and iteration was stopped after 50 improvements. The iterative algorithm is independent of the form of calculation of the spectra and is readily adapted to both the ML and EV calculations. When iteration is performed on the ML spectral estimates, the directional spectra will be referred to as the IML spectra. Similarly, an iterated EV spectra will be referred to as the IEV spectra.

3. Simulated data

Two sets of experiments on simulated spectra were performed with the intention of determining the strengths and weaknesses of the EV and IEV spectral calculations. First, the EV technique was compared to commonly used direct spectral-estimation techniques. These include the ML, the Longuet-Higgins (1963) (LH) method and a directional spectrum modeled as a cosine spread (CS):

$$E(\theta, f) = A(f)\cos^{2p}\left(\frac{\theta-\theta_0}{2}\right). \quad (15)$$

A detailed discussion of the LH and CS approaches will not be presented here, as numerous accounts appear in the literature. The coefficients p and θ_0 of the CS model can be determined from the LH coefficients as given in Hasselmann et al. (1980) as the $1M$ coefficients. Long (1980) suggested that this representation may not be appropriate over the frequencies of maximum spectral power density. Next, more detailed simulations were made to compare the data-adaptive calculations including the EV, ML, IEV and the IML methods.

To conform to the analysis of Oltman-Shay and Guza (1984), the simulations consisted of calculating a directional spectrum of the form

$$E(\theta)=\sum_{n=1}^{n_p}P_n\exp\left(-\frac{(\theta-\theta_n)^2}{2\sigma^2}\right)+E_N(\theta) \quad (16)$$

where $E_N(\theta)$ is the isotropic background noise in the signal. The noise-to-signal ratio (NSR) is defined as

$$\mathrm{NSR}=\frac{\int_0^{2\pi}E_N(\theta)d\theta}{\int_0^{2\pi}\sum P_n\exp(-(\theta-\theta_n)^2/2\sigma^2)d\theta}. \quad (17)$$

The cross-spectral matrix was then calculated using

$$Q_{ij} = \int_0^{2\pi} \beta_i \beta_j^* E(\theta) d\theta. \quad (18)$$

From the simulated cross-spectral matrix the estimated directional spectra $[\hat{E}(\theta)]$ was calculated by the four techniques outlined above. The fidelity of the estimated directional spectrum was determined from the weighted average error (WAE)

$$\text{WAE} = \frac{\int_0^{2\pi} |\hat{E}(\theta) - E(\theta)| d\theta}{\int_0^{2\pi} E(\theta) d\theta}. \quad (19)$$

A frequency of 0.1 Hz was chosen as being representative of the frequency of the spectral peak in the North Atlantic Ocean. The results were found to be insensitive to the frequency selected. The waves were assumed to be deep-water waves and the wavenumber was calculated from

$$k = \frac{\omega^2}{g}$$

The results of the simulation runs for the direct calculation appear in Table 1. The two data adaptive techniques are superior to the LH and CS calculations. Only at a NSR of 0.05 and an angular spread of 60° full width at half-maximum power (FWHP) does the CS model most closely resemble the input spectrum. The EV and ML techniques are equivalent at low NSR levels. An examination of the spectra shows that the EV technique tends to overestimate the maximum power while the ML tends to underestimate the peak power and overestimate the background noise. For increased NSR, the EV method is consistently superior to the ML technique. Figure 1 shows the directional spectrum for a NSR of 0.5 and FWHP of 30°. The EV method most accurately models the spectrum and background noise levels. The other three estimates severely underestimate the maximum power and the ML method overestimates the background noise level.

TABLE 1. Value of WAE for the direct calculations. $\Delta\theta$ is the angular full width at half maximum power (FWHP).

NSR	$\Delta\theta$	EV	ML	LH	CS
0.05	10	0.478	0.997	1.59	1.19
0.05	30	0.594	0.547	1.15	0.510
0.05	60	0.345	0.308	0.728	0.196
0.50	10	0.734	0.993	1.11	1.27
0.50	30	0.246	0.626	0.807	0.890
0.50	60	0.123	0.382	0.510	0.536
1.00	10	0.682	0.777	0.836	1.03
1.00	30	0.310	0.512	0.606	0.773
1.00	60	0.102	0.312	0.383	0.504

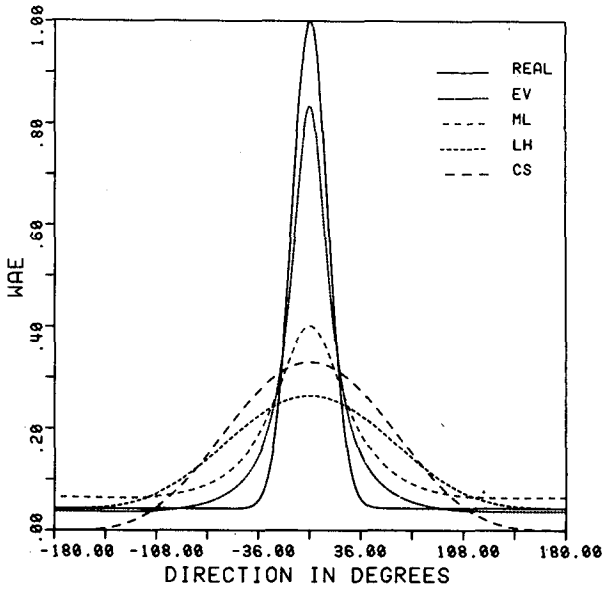

FIG. 1. Directional spectrum for the EV, ML, LH and CS techniques for a NSR of 0.5 and a FWHP of 30.0°.

Pawka (1983) and Oltman-Shay and Guza (1984) have concentrated on developing spectral estimation techniques for nearshore regions. Their studies have demonstrated the efficacy of the IML spectral estimates for waves of high signal strength (NSR of 0.1 and less) and of small angular spread (e.g. 10° full width at half-maximum power). This is quite appropriate for their purposes. First, the shoreline limits the possible fetch directions to 180°, making wave motion opposite to the peak direction impossible. Second, their instruments were located in 9.0 m of water. At this depth, even short surface gravity waves (e.g. 0.25 Hz) will be influenced considerably by bottom topography and have their wave crests refracted to align with the shore. Consequently, the results of Pawka (1983) do indicate swell peaks with an angular spread of about 10° and with very little background noise. Over the open ocean, however, one can expect much higher noise levels and much wider directional distributions. Hasselmann et al. (1980) estimate the sharpest directional distributions to have a minimum angular spread of 50° at half-maximum power. Long and Hasselmann (1979), in a simulation experiment, consider a swell peak with a full width of 20° above background noise having a NSR of 1.5. Finally, the results of Oltman-Shay and Guza (1984), simulating heave, pitch and roll data (their Fig. 13), show considerable background noise at three of four frequencies even for the near shore. Only the fourth frequency (0.059 Hz) has a noise-to-signal ratio of about 0.1 and an angular spread of about 30° at half-maximum power.

Figure 2 shows the WAE for the four data-adaptive techniques as a function of NSR for an input spectrum with a 30° angular spread at half-maximum power.

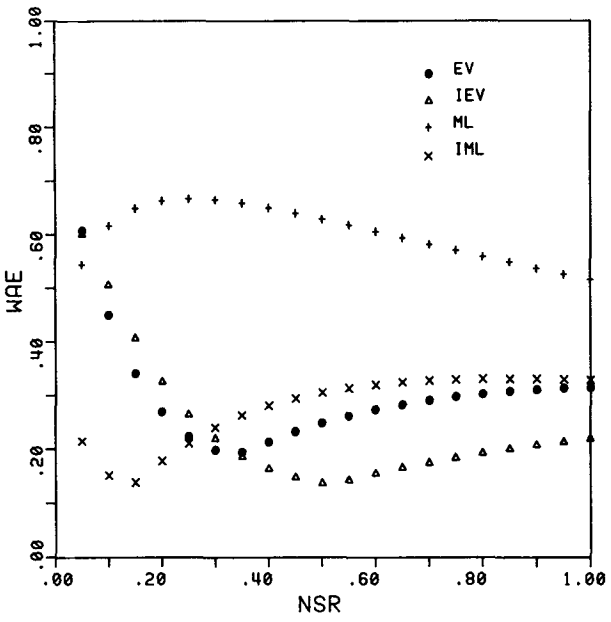

FIG. 2. Weighted average error for the IEV, EV, ML and IML techniques as a function of NSR for an input spectrum of 30° FWHP.

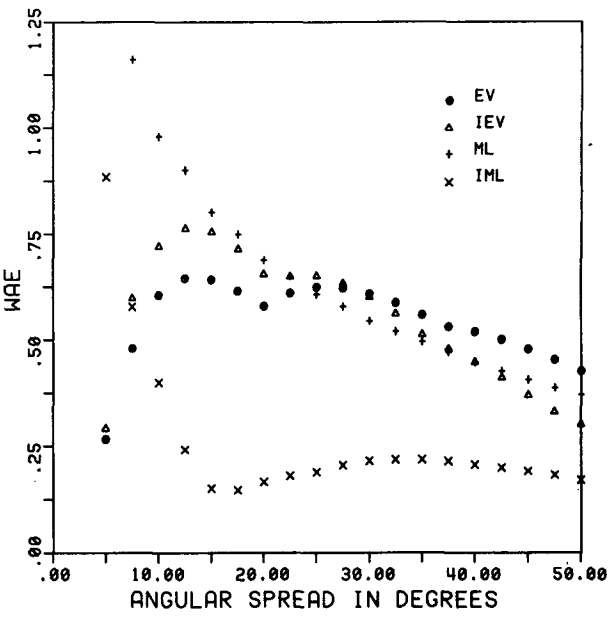

FIG. 3a. WAE for the data-adaptive techniques as a function of angular spread for a NSR of 0.05.

For a NSR of less than 0.2 the IML method is clearly superior. Above this level, the EV and IML methods have virtually identical WAE while the IEV method has a substantially lower error. Figure 3a shows a comparison of the four techniques for a NSR of 0.05 with increasing angular spread. Overall, the IML method is superior for all angular spreads. Figure 3b shows the spectra produced for NSR = 0.05 and an angular spread of 30°. The EV and IEV techniques over-resolve the simulated spectrum and produce results which overestimate the maximum power and underestimate the spectral width. Figure 4a shows the WAE for a NSR of 0.5 and varying angular spread. For angular spreads of less than 40° the IEV is clearly the superior method. Furthermore, the noniterative EV method is marginally superior to the IML technique. Figure 4b shows the predicted spectra for a NSR of 0.5 and angular spread of 30°. The IEV reproduces nearly the exact input spectrum, while the other three techniques appear to underestimate the maximum power and overestimate the spectral width.

Figure 5 shows the WAE as a function NSR for a spectrum consisting of two peaks with a FWHP of 30° separated by 120°. The IEV method is clearly superior to the other techniques and is most accurate in the low NSR regime. Figure 6a shows the WAE for increasing angular spread for a NSR = 0.05. The IEV produces small errors for small values of the FWHP. Figure 6b shows an example of the predicted spectrum for NSR = 0.05, FWHP = 30° and an angular separation of 120°. The IEV predicts the spectral peaks and the spectral gap most accurately. Figure 7a shows the WAE as a function of increasing spectral width for a NSR of 0.5, while Fig. 7b gives an example of the specific spectrum for an angular spread of 30°. Here, none of the predicted spectra are particularly accurate as all methods tend to underestimate the spectral peaks. Again the IEV method yields the best estimate. The angular separation was also varied for a bimodal distribution for NSR = 0.05 with an angular spread of 30°. Results similar to Oltman-Shay and Guza (1984) were found.

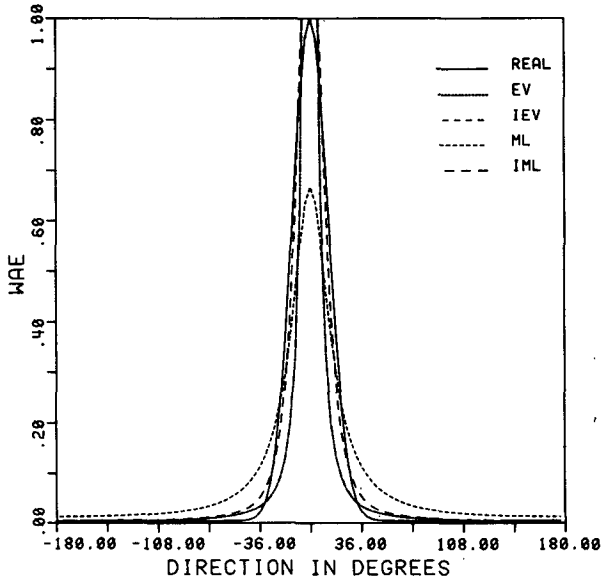

FIG. 3b. Example of the directional spectrum for a NSR of 0.05 and 30° FWHP.

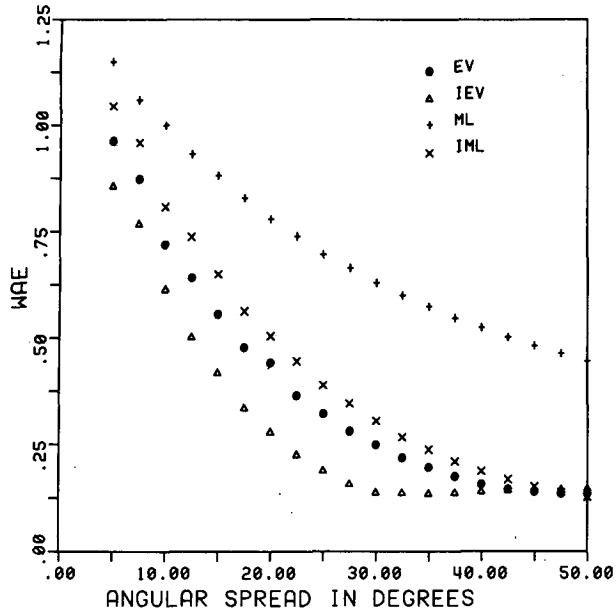

FIG. 4a. As in Fig. 3a but for a NSR of 0.5.

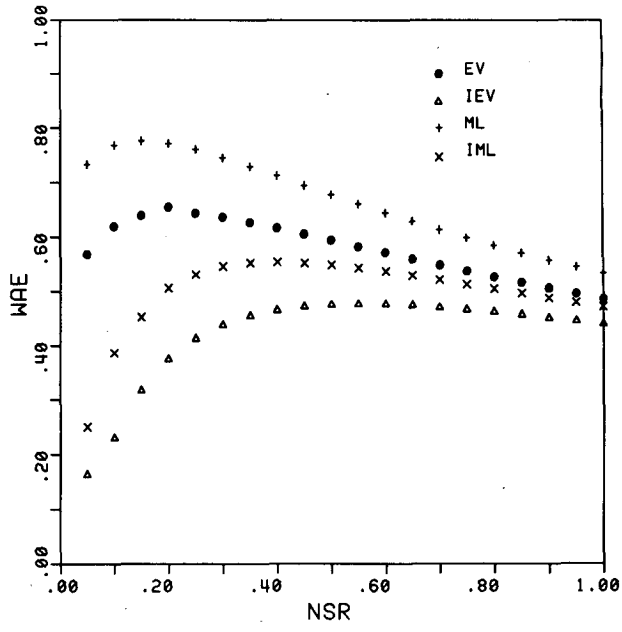

FIG. 5. WAE as a function of NSR for a spectrum consisting of two peaks with a FWHP of 30° separated by 120°.

For separations less than 60° the two peaks could not be detected by any method. For separations greater than 60° both peaks could be resolved at the correct peak directions.

The stability of the estimation technique to input stochastic errors in the cross-spectral matrix was tested following the method of Brennan and Mallet (1976). As in Oltman-Shay and Guza (1984), 50 estimates of a cross-spectral matrix with 30 degrees of freedom were made. The input deterministic spectrum had a unit amplitude at a peak direction of 0.0°, FWHP = 30° and a NSR of 0.5. As in Long and Hasselmann (1979) it is assumed that at least part of the background noise level is of physical, and not stochastic, origin. The mean and standard deviations of the peak direction and the peak amplitude were calculated and are shown in Table 2. The peak directions were virtually identical for all methods. All produced a mean peak direction near 0.0° and a standard deviation of about 7.0°. The estimated amplitudes for the ML, IML and EV techniques are biased low (as one expects from the deterministic results, see Fig. 4b). The IEV results show a maximum power at the peak direction very close to the input 1.0. The standard deviation of the EV, IEV and IML results are somewhat larger than for the ML method. The maximum amplitude, however, has as a lower limit, the input energy is divided by the bandwidth, and hence for similar stability one expects lower standard deviations for lower mean amplitudes. All techniques exhibit a similar stability and direction. The IEV technique, however, also reproduces the correct mean maximum amplitudes.

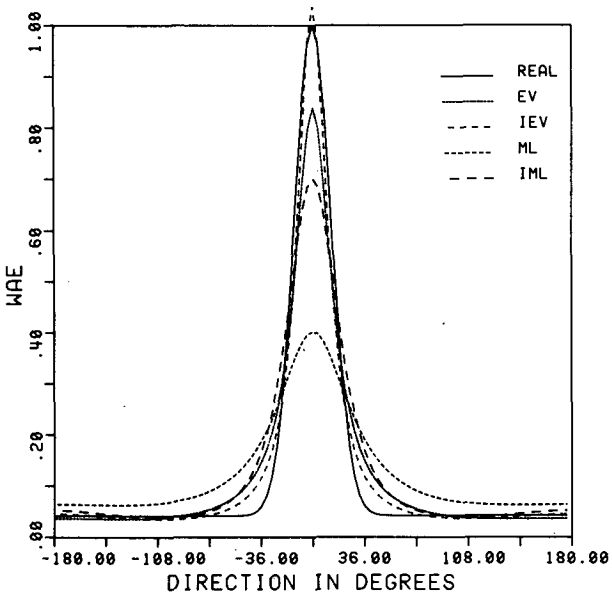

FIG. 4b. As in Fig. 3b but for a NSR of 0.5.

4. Real data

The spectral estimation methods were used to detect the directional spectrum from heave, pitch and roll data collected during a Canadian Environmental Studies Revolving Fund intercomparison study of directional spectra estimates sampled on the Grand

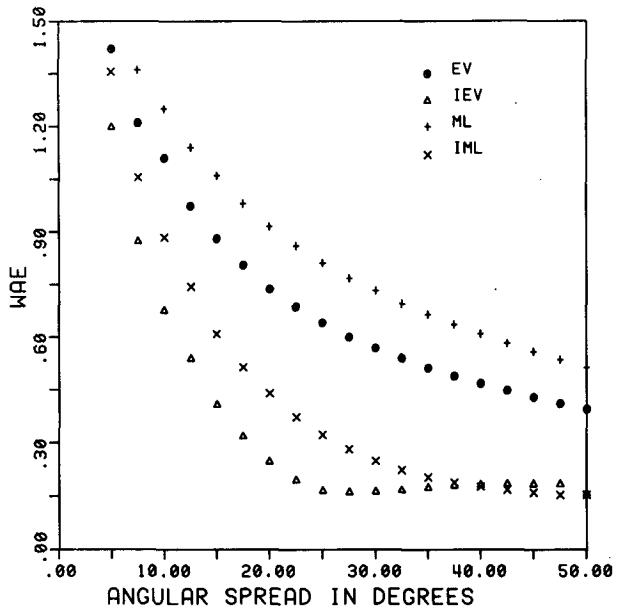

FIG. 6a. WAE as a function of angular spread for a bimodal spectrum with a NSR of 0.05 and an angular separation of 120°.

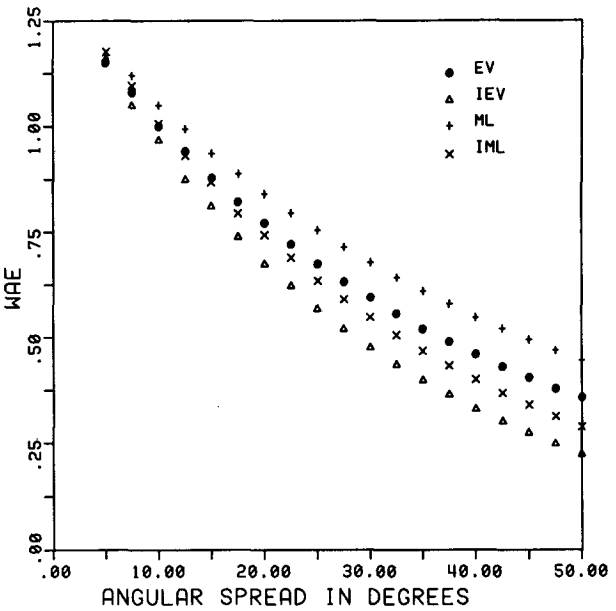

FIG. 7a. As in Fig. 6a but with NSR of 0.50.

Banks of Newfoundland, Canada at the location shown in Fig. 8. The wave-detection instrument was a Datawell Wavec heave, pitch and roll buoy which was moored in 85 m of water. It sampled at 1.28 Hz for 34 minute bursts every three hours. For this study, each 34 minute burst was divided into 20 groups of 128 data points, giving a frequency resolution of 0.01 Hz and 40 degrees of freedom. Further details of instrument deployment and data collection can be found in Juszko (1985).

The directional spectra were calculated from the cross-spectral matrix according to methods outlined in preceding sections and then were inverted to construct a vector (**b**) of model cross-spectral entries according to

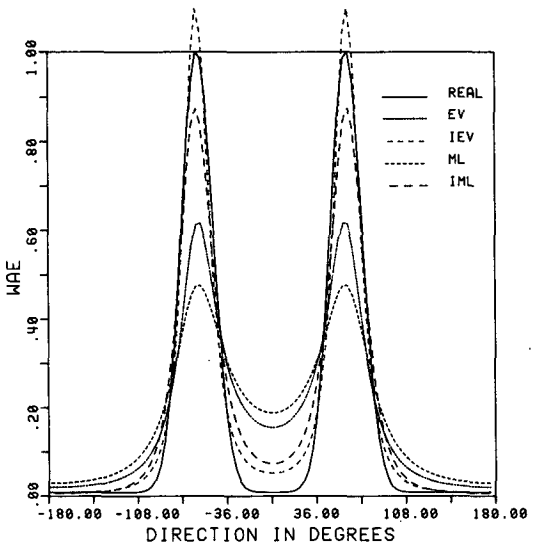

FIG. 6b. Example of a bimodal spectrum with a NSR of 0.05, FWHP of 30° and an angular separation of 120°.

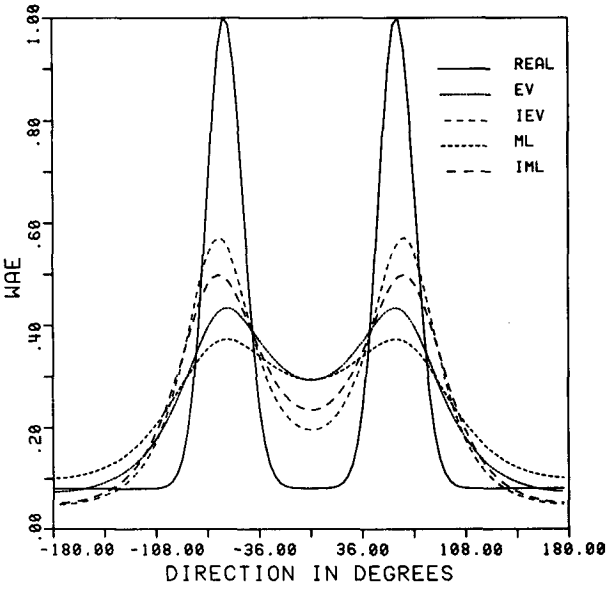

FIG. 7b. As in Fig. 6b but with a NSR of 0.5.

TABLE 2. Comparison of peak direction and peak angle for a simulation of stochastic errors for an input spectrum of unit peak amplitude with a peak direction of 0.0°, full width at half power of 30° and a NSR of 0.5.

Method	EV	IEV	ML	IML
Peak direction	$-1.72 \pm 6.76°$	$-1.72 \pm 7.22°$	$2.30 \pm 7.24°$	$2.30 \pm 7.33°$
Peak amplitude	0.79 ± 0.41	0.96 ± 0.51	0.43 ± 0.17	0.70 ± 0.32

$$\mathbf{b} = \begin{pmatrix} C_{11} \\ C_{12} \\ Q_{12} \\ C_{13} \\ Q_{13} \\ C_{22} \\ C_{23} \\ Q_{23} \\ C_{33} \end{pmatrix} = \hat{C}_{11} \begin{pmatrix} 1.0 \\ 0.0 \\ -\int_0^{2\pi} k\cos(\theta)\hat{E}(\theta)d\theta \\ 0.0 \\ -\int_0^{2\pi} k\sin(\theta)\hat{E}(\theta)d\theta \\ \int_0^{2\pi} k^2\cos^2\hat{E}(\theta)d\theta \\ \int_0^{2\pi} k^2\cos(\theta)\sin(\theta)\hat{E}(\theta)d\theta \\ 0.0 \\ \int_0^{2\pi} k^2\sin^2(\theta)\hat{E}(\theta)d\theta \end{pmatrix} \quad (20)$$

where C represents the model cospectral value, Q represents the model quadspectral value and the subscripts refer to the amplitude and tilt channels. Following Long (1980), the wavenumber was estimated from

$$k = \left(\frac{\hat{C}_{22} + \hat{C}_{33}}{\hat{C}_{11}}\right)^{1/2} \quad (21)$$

where the careted variables indicate data values. This was found to give more stable estimates of the directional spectrum than inverting the surface gravity wave dispersion relation. Juszko (1985) has shown that the two estimates of the wavenumber agree on average for moderate wind conditions. Letting $\hat{\mathbf{b}}$ be the vector of data cross-spectral values, an estimate of the error in the model cross-spectral values is given by

$$\rho^2 = \mathbf{e}\mathbf{V}^{-1}e \quad (22)$$

where $\mathbf{e} = \mathbf{b} - \hat{\mathbf{b}}$ and $\mathbf{V}$ is the variance of the model cross-spectral estimates. A derivation of the expected errors for this matrix can be found in Jenkins and Watts (1969). In practice, Eq. (11) of Long (1980) was used to estimate the entries. For small errors, ρ^2 follows a χ^2 distribution. The normalization of the total model power spectral density to $\hat{C}_{11}$ and the implementation

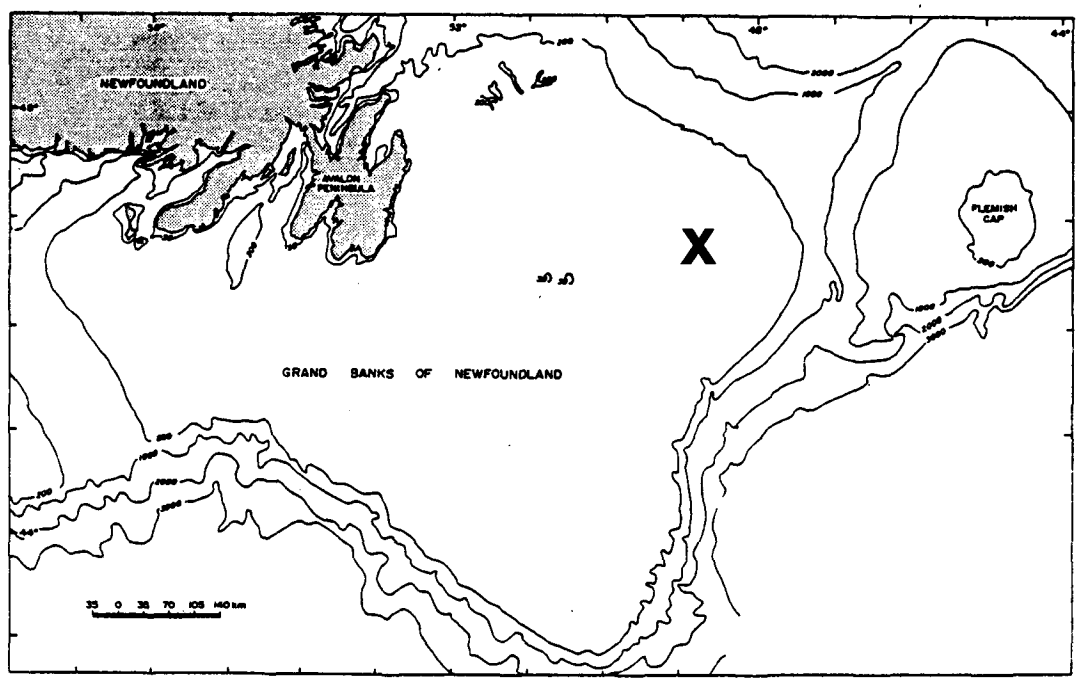

FIG. 8. Location of ESRF intercomparison study.

of (21) reduce the nine cross-spectral entries to seven degrees of freedom. Lawson and Long (1983) use ρ^2 as a criterion of performance for the iteration to their directional spectra. They set the 80% probability zone as an acceptable level of error. This means that there is a 20% probability that an acceptable model fails to meet the χ^2 criterion. For seven degrees of freedom, any value of $\rho^2 < 9.8$ lies within the 80% confidence zone of the particular model. In effect, ρ^2 acts as a residual error estimate for the cross-spectral matrix and can be used to assess the effectiveness of the model directional spectrum in accounting for the data and allows an intercomparison between our results and those of Lawson and Long (1983).

One possible scenario for the development of wave propagation in two directions at the same frequency occurs during storm build-up. The wave spectra could be composed of a swell originating remote from the sampling location and of a directly forced sea arising from local winds. Fig. 9(a) shows a heave spectrum, 9(b) the ρ^2 for each of the four direct methods, and 9(c) ρ^2 for the data adaptive methods. Two peaks are evident—at 0.1 Hz and at 0.2 Hz. The 80% confidence level is indicated by the horizontal line in Figs. 9(b) and 9(c). Over the regions of large spectral power density the CS values of ρ^2 exceed the bounds of the graph. The LH method reasonably models the low-frequency peak, but its errors fall well outside the 80% confidence interval for the high-frequency peak. The ML error is smaller than for the LH and CS estimates, but it is consistently larger than the EV method particularly over the high-frequency regime. Finally, the confidence level of the EV method compares favorably with the results achieved by the iterative procedure of Lawson and Long (1983). Figure 9(c) shows the same calculation for the data-adaptive techniques. The iterative IML and IEV methods show nearly identical errors. Except for two frequency bands, these results are well within the 80% confidence band.

Figure 10 shows typical directional spectra calculated over the two maxima in the power spectra of Fig. 9. At 0.10 Hz all the data adaptive analyses clearly indicate two spectral peaks. The IEV method, however, has the smallest error and shows the sharpest resolution of the two peaks. The NSR is estimated at 0.5 and the simulation runs indicate that the peaks are probably underresolved. At 0.20 Hz, the IEV method produces a narrower peak than the other three methods. The spectral width from the EV, IEV and IML techniques indicates that the wave field has an FWHP of about 20.0°. The NSR for this peak is estimated at between 0.2 and 0.3. The error in the cross-spectral matrix is similar between the EV, IEV and IML methods, again in agreement with the simulation runs.

5. Summary and conclusions

A new data-adaptive technique for the analysis of heave, pitch and roll buoy data has been presented.

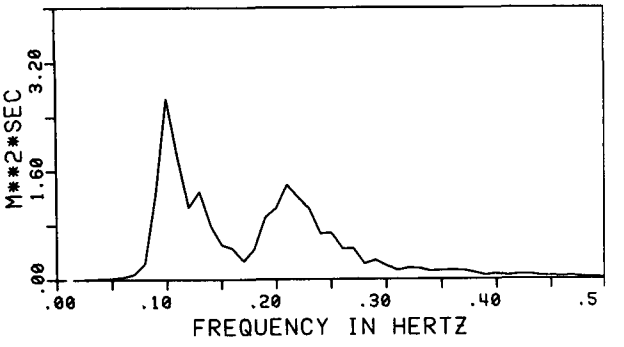

FIG. 9a. Heave spectrum during a storm development.

The data cross-spectral matrix is diagonalized and the eigenvectors corresponding to the two smallest eigenvalues are assumed to span the noise of the measurement, and the eigenvector corresponding to the largest eigenvalue is assumed to span the signal. The directional spectrum is then determined from the noise component. If the three eigenvectors are used to determine the directional spectrum, then the method is identical to the maximum likelihood spectral estimate.

The eigenvector technique was compared to other directly calculated spectral estimates, including the maximum likelihood estimate, the Longuet-Higgins et al. (1963) estimate and the cosine spread model. In the

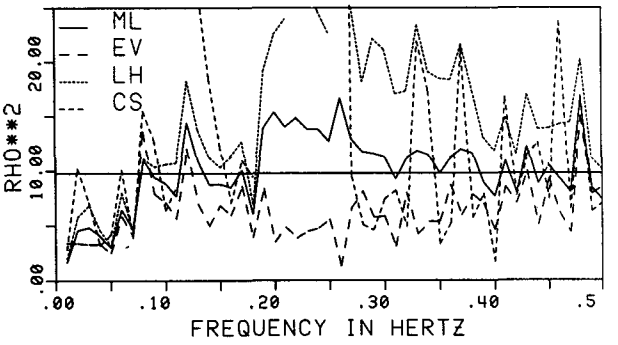

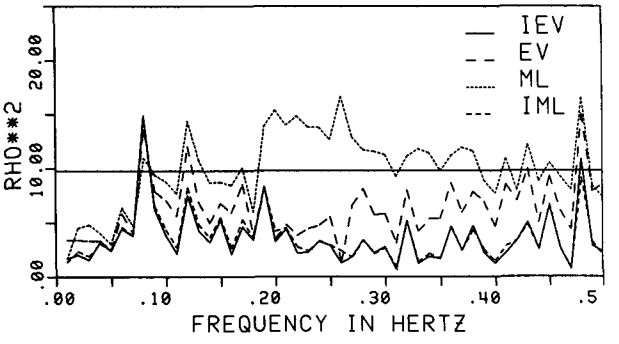

FIG. 9b. Value of ρ^2 for the direct spectral estimation techniques.
FIG. 9c. Value of ρ^2 for the data adaptive spectral estimation techniques.

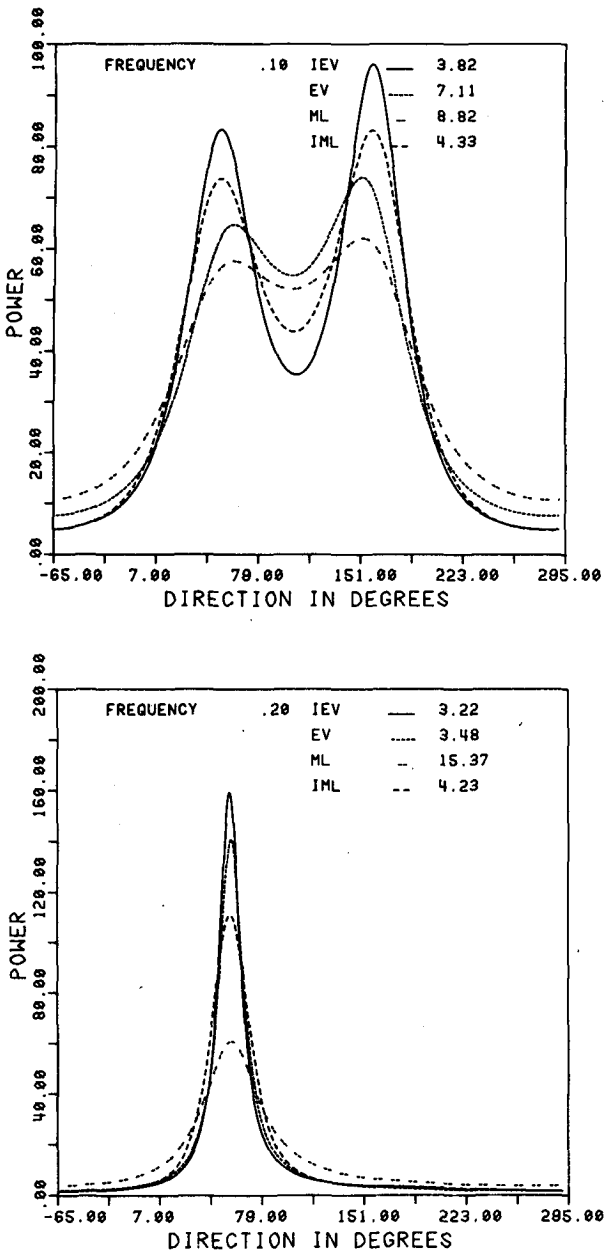

FIG. 10. Examples of unimodal and bimodal spectra calculated by the data adaptive techniques.

simulation experiments, the eigenvector method overall proved superior to all other direct calculations, for all noise-to-signal ratios and for all angular spreads. With real data, the error in the cross-spectral matrix was used as an indicator of goodness-of-fit. Again, the eigenvector method was clearly superior to the other methods tested. Furthermore, the error in the cross-spectral matrix was within the 80% confidence limits which form the basis of the iteration method of Lawson and Long (1983).

An iterative version of the eigenvector method was calculated according to the technique of Pawka (1983). The results were compared to the eigenvector, the maximum likelihood and the iterative maximum likelihood estimates. In the simulation tests, for a single-peak spectrum with a spread of 30° full width at half-maximum, there was a definite demarcation in accuracy. For the high-signal regime (noise-to-signal ratio less than 0.20), the iterative maximum likelihood estimate was superior. The eigenvector and iterative eigenvector methods overestimated the peak power. For a noise-to-signal ratio greater than 0.20, the eigenvector and iterative eigenvector methods produced lower weighted-average errors. For a double-peaked spectrum, the iterative eigenvector method was superior at all noise levels tested.

The four data-adaptive methods were also tested for simulated stochastic noise in the cross-spectral matrix. The average of fifty simulated cross-spectral matrices, each with 30 degrees of freedom, indicated virtually no difference in stability among the four data-adaptive methods. The mean direction and peak amplitudes were, on average, as predicted by the simulated spectra.

The iterative methods were also tested on real data using the error in the predicted cross-spectral matrix to indicate model significance. The two iterative methods produced errors well below the 80% confidence limits. For a double-peaked spectrum, the iterative eigenvector method showed the lowest error and most clearly defined the two peaks and the spectral gap. For the single peak, the error in the eigenvector, the iterative eigenvector and the iterative maximum likelihood techniques were nearly identical. It must be emphasized that these results are representative not only of the small sample presented but also of more than 350 spectra examined. In short, the eigenvector and iterative eigenvector methods give superior estimates of wave-directional spectra in the moderate noise situations that can be expected over the open ocean.

Acknowledgments. Discussions with Drs. M. Wilmut and F. Milinazzo of the Mathematics Department at RRMC are appreciated. RFM received support from Chief of Research and Development Grant RR15 from the Department of National Defence of Canada.

REFERENCES

Barrodale, I., M. Greening and C. Zala, 1985: An indepth study of the eigenvector method for high-resolution beamforming. Defence Research Establishment Pacific-Contractors Report 85-7. 65 pp.

Brennan, L. E., and J. D. Mallet, 1976: Efficient simulation of external noise incident on arrays. *IEEE Trans. Antenn. Propag.*, **24**, 740–741.

Capon, J., 1969: High-resolution frequency-wave-number spectrum analysis. *Proc. IEEE*, **57**, 1408–1418.

Davis, R. E., and L. A. Regier, 1977: Methods for estimating directional wave spectra from multi-element arrays. *J. Mar. Res.*, **35**, 453–477.

Hasselmann, D. E., M. Dunckel and J. A. Ewing, 1980: Directional wave spectra observed during JONSWAP 1973. *J. Phys. Oceanogr.*, **10,** 1264–1280.

Jenkins, G. M., and D. G. Watts, 1968: *Spectral Analysis and Its Application.* Holden-Day, 525 pp.

Johnson, D. H., 1982: The application of spectral estimation methods to bearing estimation problems. *Proc. IEEE,* **70**(9), 1018–1028.

Juszko, B-A., 1985: Comparison of Directional Wave Spectra. 090-17-08 available from Canada Oil and Gas Lands Administration. 148 pp.

Kanasewich, E. R., 1981: *Time Sequence Analysis in Geophysics,* Third Ed. The University of Alberta Press, 480 pp.

Lawson, L. M., and R. B. Long, 1983: Multimodal properties of the surface-wave field observed with pitch-roll buoys during GATE. *J. Phys. Oceanogr.*, **13,** 474–486.

Long, R. B., 1980: The statistical evaluation of directional spectrum estimates derived from pitch/roll buoy data. *J. Phys. Oceanogr.*, **10,** 944–952.

——, and K. F. Hasselmann, 1979: A variational technique for extracting directional spectra from multi-component wave data. *J. Phys. Oceanogr.*, **9,** 373–381.

Longuet-Higgins, M. S., D. E. Cartwright and N. D. Smith, 1963: Observations of the directional spectrum of sea waves using the motion of a floating buoy. *Ocean Wave Spectra,* Prentice Hall, 111–136.

Oltman-Shay, J., and R. T. Guza, 1984: A data-adaptive ocean wave directional-spectrum estimator for pitch and roll type measurements. *J. Phys. Oceanogr.*, **14,** 1800–1810.

Pawka, S. S., 1983: Island shadows in wave directional spectra. *J. Geophys. Res.*, **88,** 2579–2591.

——, D. L. Inman and R. T. Guza, 1984: Radiation stress estimators. *J. Phys. Oceanogr.*, **13,** 1698–1708.